Supplementary Material (ESI) for CrystEngComm
This journal is © The Royal Society of Chemistry

A Series of 0D to 3D Anderson-type Polyoxometalate-based Compounds Obtained under Ambient and Hydrothermal Conditions

Jun Ying,[†] Ya-Guang Chen*,[†] and Xiu-Yan Wang[†]

Table S1. Selected bond distances (Å) and angles (°) for compounds **1–7**.

Compound **1**			
Cu1-N1	2.001(3)	Cu1-N2	2.018(3)
Cu1-O19	2.352(2)	Cu2-N3	1.994(3)
Cu2-N5	2.005(3)	Cu2-N4	1.995(3)
Cu2-N6	2.002(3)	Cu2-O9	2.592(4)
Cu2-O4	2.810(3)	N1-Cu1-N1	180.0
N1-Cu1-N2	85.21(15)	N1-Cu1-N2	94.80(15)
N2-Cu1-N2	180.0	N3-Cu2-N5	174.95(13)
N3-Cu2-N4	94.83(13)	N5-Cu2-N4	84.29(13)
N3-Cu2-N6	85.16(13)	N5-Cu2-N6	95.30(12)
N4-Cu2-N6	175.22(15)		
Symmetry codes for **1:** #1 -x+3/2,-y+3/2,-z+1		#2 -x+2,-y+1,-z+1	#3 -x+2,-y,-z+1
Compound **2**			
Cu1-N2	2.001(4)	Cu1-N4	2.006(4)
Cu1-N3	2.002(4)	Cu1-N1	2.007(4)
Cu1-O1	2.602(3)	Cu1-O2	2.802(4)
Cu2-N6	2.005(4)	Cu2-N6	2.005(4)
Cu2-O17	2.361(3)	Cu2-N5	2.028(4)
N2-Cu1-N3	94.95(17)	N2-Cu1-N4	175.07(18)
N2-Cu1-N1	84.21(17)	N4-Cu1-N3	85.16(16)
N3-Cu1-N1	175.47(16)	N4-Cu1-N1	95.30(16)
N6-Cu2-N5	94.71(19)	N6-Cu2-N6	180.0
N6-Cu2-N5	85.29(19)	N6-Cu2-N5	180.0
N5-Cu2-N5	180.0	N6-Cu2-N5	94.70(19)
Symmetry codes for **2:** #1 -x+3/2,-y+3/2,-z+1		#2 -x+1,-y+2,-z+1	#3 -x+1,-y+3,-z+1
Compound **3**			
Cu3-N3	1.907(15)	Cu3-N4	2.150(18)
Cu3-O6	2.513(8)	Cu2-O13	1.937(8)
Cu2-O13	1.960(9)	Cu2-N2	1.973(10)
Cu2-N1	1.987(10)	Cu2-O7	2.679(11)
Cu2-O8	2.504(14)	N3-Cu3-N3	180.0
N3-Cu3-N4	80.2(6)	N3-Cu3-N4	99.8(6)
N4-Cu3-N4	180.0	O13-Cu2-O13	83.4(3)
O13-Cu2-N2	176.4(4)	O13-Cu2-N2	95.3(4)
O13-Cu2-N1	94.6(4)	O13-Cu2-N1	172.1(4)

N2-Cu2-N1	87.1(5)		
Symmetry codes for **3:** #1 -x,-y+2,-z+1 #2 -x,-y+1,-z+1 #3 -x-1,-y,-z+2			
Compound **4**			
O1W-Cu1	2.343(4)	Cu1-N6	1.995(5)
Cu1-N1	1.994(5)	Cu1-N10	2.006(5)
Cu1-N7	2.026(5)	Cu1-O8	2.607(4)
N6-Cu1-N1	88.08(19)	N6-Cu1-N10	90.83(19)
N1-Cu1-N10	174.0(2)	N6-Cu1-N7	174.0(2)
N1-Cu1-N7	92.01(19)	N10-Cu1-N7	88.45(19)
N6-Cu1-O1W	88.94(18)	N1-Cu1-O1W	93.52(19)
N10-Cu1-O1W	92.37(19)	N7-Cu1-O1W	97.07(18)
Symmetry codes for **4:** #1 x+1,y,z #2 x-1,y,z			
Compound **5**			
Cu1-N4	1.989(3)	Cu1-O1W	2.009(2)
Cu1-O2W	2.327(2)	Cu2-O8	1.932(2)
Cu2-O20	1.939(2)	Cu2-N1	1.949(3)
Cu2-O3	1.956(2)	Cu2-O6	2.737(4)
N4-Cu1-N4	180.0(8)	Cu2-O7	2.814(4)
N4-Cu1-O1W	91.09(11)	N4-Cu1-O1W	88.91(11)
O1W-Cu1-O1W	180.0 (8)	N4-Cu1-O1W	88.90(11)
O1W-Cu1-O2W	88.78(10)	N4-Cu1-O2W	90.64(10)
N4-Cu1-O2W	89.36(10)	O1W-Cu1-O2W	89.78(10)
O8-Cu2-N1	169.86(12)	O8-Cu2-O20	92.11(10)
O8-Cu2-O3	85.72(9)	O20-Cu2-N1	92.00(11)
N1-Cu2-O3	89.96(11)	O20-Cu2-O3	177.55(10)
Symmetry codes for **5:** #1 -x,-y,-z+1 #2 -x+1,-y+1,-z+2 #3 -x,-y+1,-z+2 #4 -x-1,-y-1,-z+1			
Compound **6**			
O1-Cu1	2.132(3)	O2-Cu1	2.255(2)
Cu1-N1	1.946(3)	Cu1-N3	1.955(3)
K1-O4	2.046(3)	K1-O1W	2.091(4)
K1-O7	2.331(3)	N1-Cu1-N3	146.09(13)
N1-Cu1-O1	101.47(12)	N3-Cu1-O1	102.51(12)
N1-Cu1-O2	99.47(11)	N3-Cu1-O2	100.90(11)
O1-Cu1-O2	97.24(10)		
Symmetry codes for **6:** #1 -x+3,-y-1,-z+1 #2 -x+4,-y-1,-z+1 #3 -x+4,y,-z+3/2 #4 x,y-1,z #5 -x+3,y,-z+3/2 #6 x,y+1,z			
Compound **7**			
Cd1-O4W	2.034(9)	Cd1-O1W	2.043(9)
Cd1-N6	2.103(10)	Cd1-O3W	2.090(8)
Cd1-O5W	2.105(8)	Cd1-O2W	2.175(10)
Cd2-O7W	2.071(8)	Cd2-N1	2.168(11)
Cd2-O6W	2.107(8)	O4W-Cd1-O1W	93.3(4)

O5W-Cd1-O2W	86.0(4)	O3W-Cd1-O2W	87.0(4)
N6-Cd1-O2W	177.0(4)	O1W-Cd1-O2W	88.2(4)
O4W-Cd1-O2W	90.2(4)	O3W-Cd1-O5W	86.7(4)
N6-Cd1-O5W	94.1(4)	O1W-Cd1-O5W.	173.7(4)
O4W-Cd1-O5W	89.3(4)	N6-Cd1-O3W	90.0(4)
O1W-Cd1-O3W	90.5(4)	O4W-Cd1-O3W	175.2(4)
O1W-Cd1-N6	91.5(4)	O4W-Cd1-N6	92.8(4)
Symmetry codes for **7:** #1 -x,-y+1,-z		#2 -x,-y,-z+1	

Table S2. CAT% data of **6**–CPE for reduction of $KBrO_3$, NO_2^-, H_2O_2 and oxidation of AA.

Concentration of the substrate	Substrate			
	$KBrO_3$	NO_2^-	H_2O_2	AA
2 mM	14.5	59.5	32.6	98.2
4 mM	55.6	100.2	80.2	524.7
6 mM	83.7	137.1	153.3	831.2
8 mM	149.8	191.1	219.9	1008.0

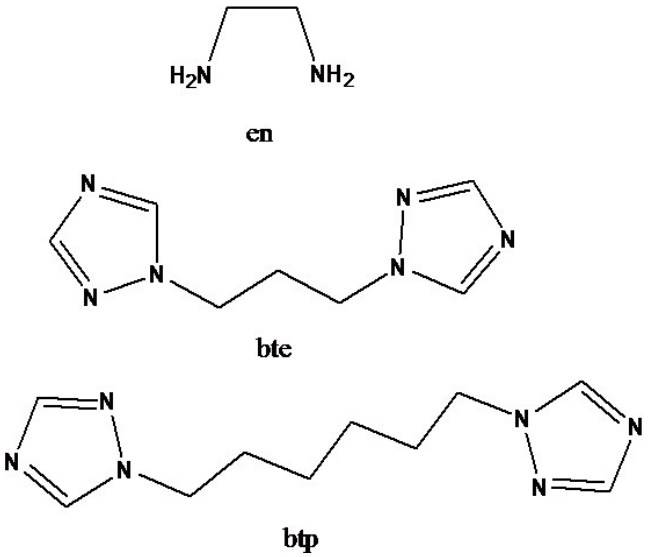

Scheme S1. Three ligands used in this work: ethanediamine (en), 1,2-bis(1,2,4-triazol-1-yl)ethane (bte) and 1,3-bis(1,2,4-triazol-1-yl)propane (btp).

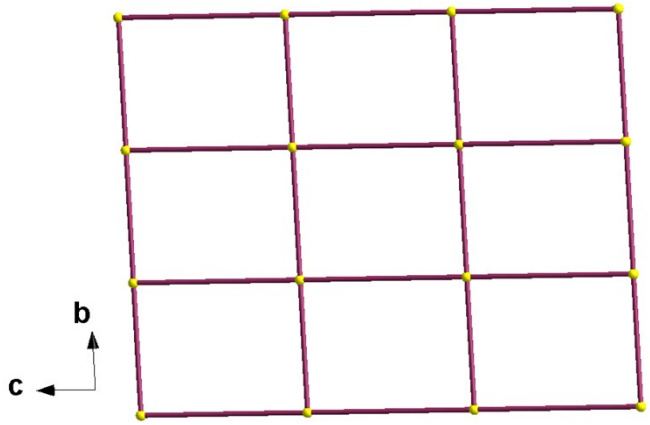

Fig. S1. The schematic view of 2D grid-like of compound **3**.

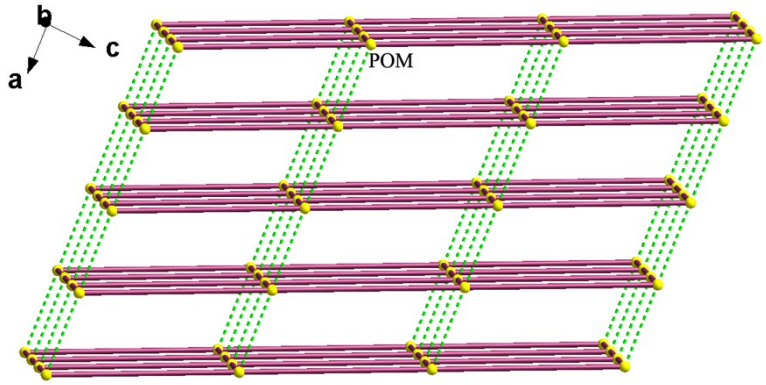

Fig. S2. The 3D supramolecular structure of **3** with adjacent layers linked by hydrogen bonding interactions.

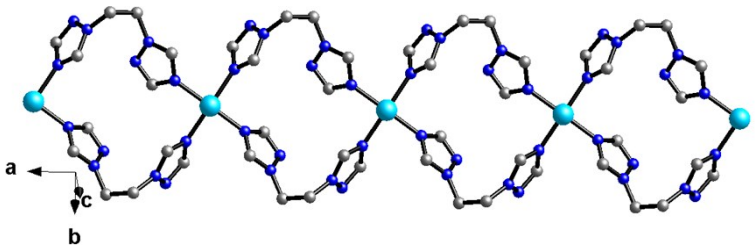

Fig. S3. The 1D cycle-connecting-cycle metal-organic chain in compound **4**.

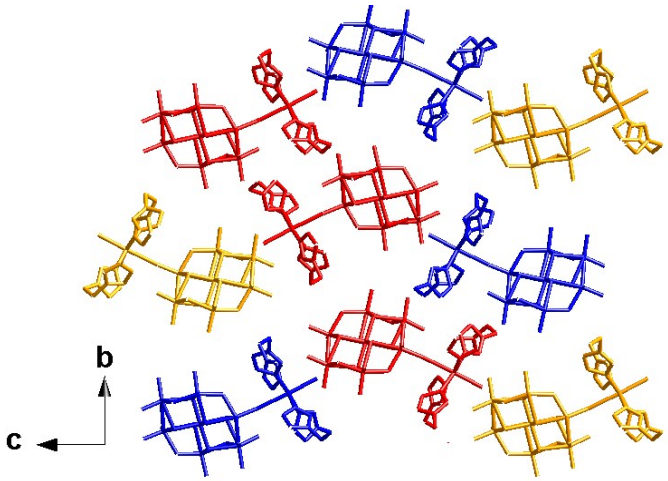

Fig. S4. The 3D supramolecular structure of compound **4** with adjacent chains lined by hydrogen bonding interactions.

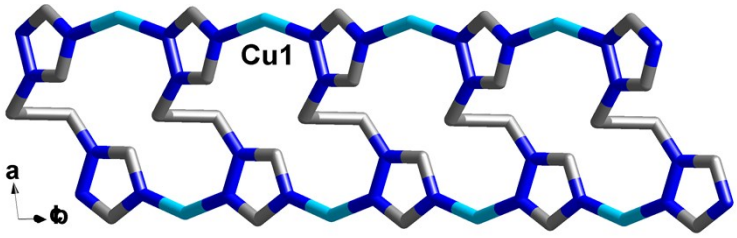

Fig. S5. The ladder-like Cu-btp chain with btp as crossing bars of compound **6**.

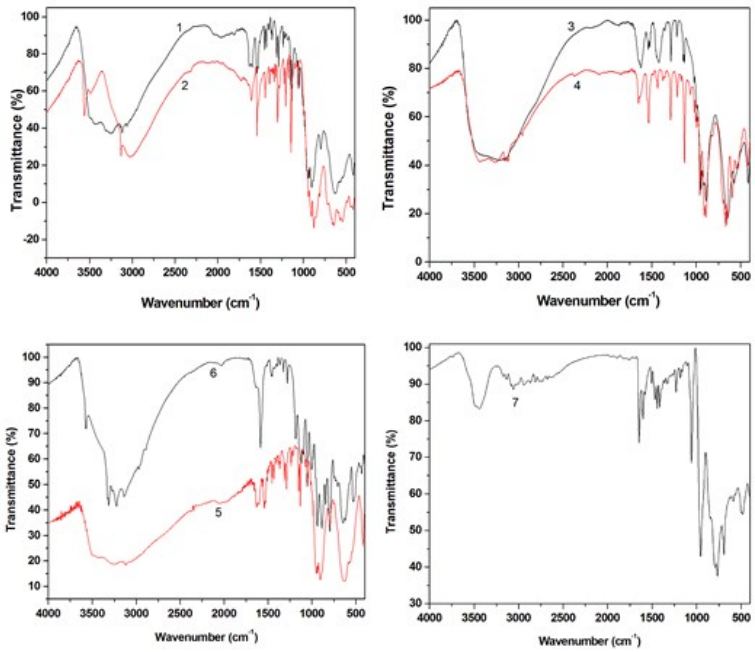

Fig. S6. The IR spectra of compounds **1**–**7**.

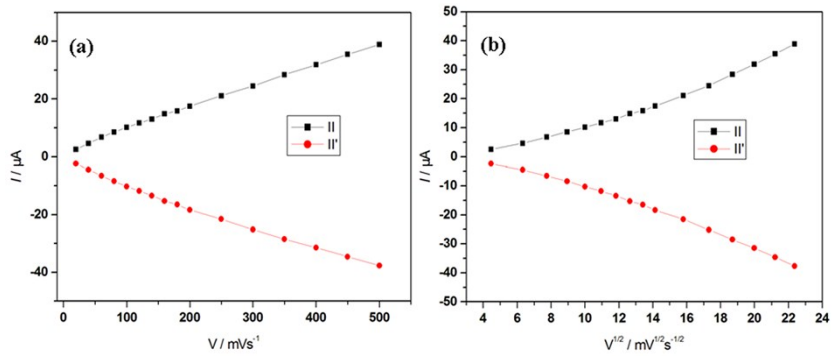

Fig. S7. (a), (b): Plots of the anodic and the cathodic peak II–II′ current against υ and $\upsilon^{1/2}$.

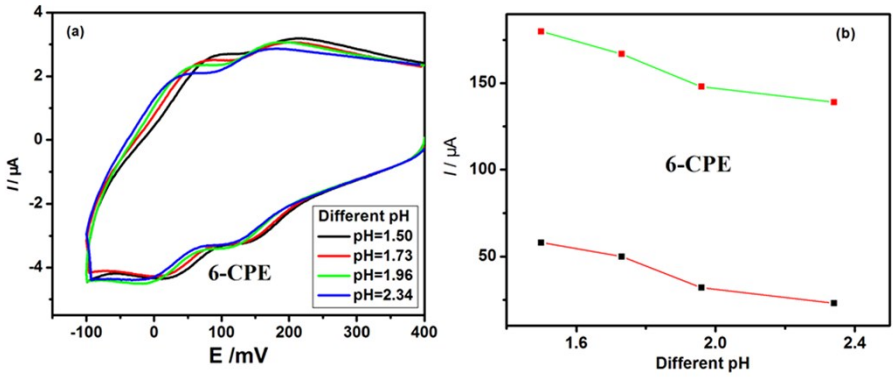

Fig. S8. Cyclic voltammograms of the **6**–CPE in $H_2SO_4 + Na_2SO_4$ aqueous solution with different pH. Scan rate: 200 $mV \cdot s^{-1}$.

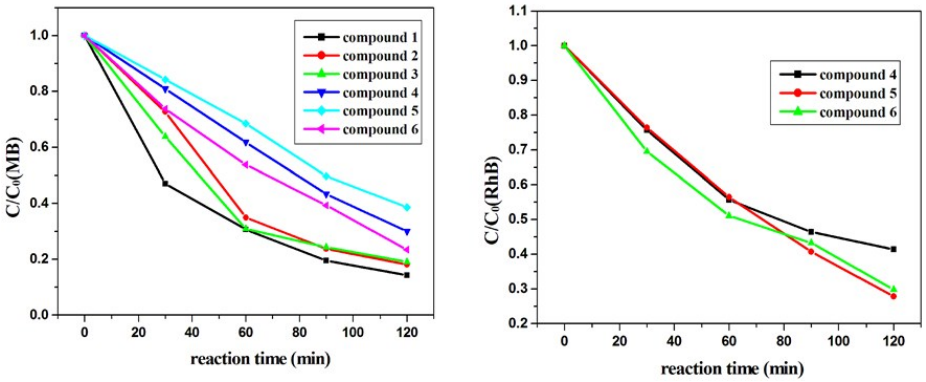

Fig. S9. The conversions of MB and RhB with the compounds **1**–**6** as the catalysts.